Intrinsic ferromagnetism in CeO_2: dispelling the myth of vacancy site localization mediated superexchange

2009 J. Phys.: Condens. Matter 21 405502

(http://iopscience.iop.org/0953-8984/21/40/405502)

J. Phys.: Condens. Matter **21** (2009) 405502 (6pp) doi:10.1088/0953-8984/21/40/405502

Intrinsic ferromagnetism in CeO_2: dispelling the myth of vacancy site localization mediated superexchange

P R L Keating, D O Scanlon and G W Watson

School of Chemistry, Trinity College Dublin, Dublin 2, Republic of Ireland

E-mail: scanloda@tcd.ie and watsong@tcd.ie

Received 30 July 2009, in final form 23 August 2009
Published 14 September 2009
Online at stacks.iop.org/JPhysCM/21/405502

Abstract

Intrinsic ferromagnetism in CeO_2 is a source of controversy in the literature and has been linked to the excess electrons left over upon oxygen vacancy formation on Ce sites neighbouring the vacancy. A recent theoretical study (Han *et al* 2009 *Phys. Rev.* B **79** 100403) concluded that increased vacancy concentration changes the localization behaviour of CeO_2, resulting in some degree of charge localization in the vacancy site itself, which leads to superexchange and polarization effects that enhance the stability of ferromagnetism. In this report, we show conclusively that oxygen vacancy concentrations of up to 12.5% *do not* cause localization in the vacancy site, and that this *is not* responsible for any enhanced ferromagnetism. Investigation of oxygen vacancies on the (111), (110) and (100) low index surfaces also show no evidence for ferromagnetic preference.

(Some figures in this article are in colour only in the electronic version)

1. Introduction

The localization of electrons and ordering of spins in oxides has enjoyed an explosion of interest recently, with studies in the field of spintronics and dilute magnetic semiconductors (DMS) becoming increasingly common [1]. Transition metal (TM) doping of metal oxides was first postulated by Dietl *et al* as a method of inducing ferromagnetic (FM) behaviour [2]. This sparked many experimental and theoretical studies of TM doping of non-magnetic oxides, but to date the field still remains controversial [3–5]. Even *more* controversial is the FM behaviour reported in *undoped* thin films of non-magnetic metal oxides [6–8]. This was first reported by Coey and co-workers in thin films of HfO_2 [6], and has been related to the formation of both anion [9] and cation [7] vacancies. Subsequently, a conflicting report attributed the FM behaviour to contamination by iron, caused by the handling of the thin films by stainless steel tweezers [8]. Despite this controversy, ferromagnetic behaviour has been reported for thin films of TiO_2 and In_2O_3 [10] and in nanoparticles of Al_2O_3, ZnO, SnO_2, In_2O_3 and CeO_2 [11].

CeO_2 is at present one of the key materials in this environmentally conscious age, having applications in intermediate temperature solid oxide fuel cells (IT-SOFCs) [12], and in preferential CO oxidation, catalytic oxidation of hydrocarbons, and especially in three-way catalysts (TWCs) [13]. Ceria's importance stems from its oxygen storage capability (OSC), which allows it to release oxygen under reducing conditions and to store oxygen by filling oxygen vacancies under oxidizing conditions. Stoichiometric CeO_2 is paramagnetic, however the formation of an oxygen vacancy is known to result in the donation of two electrons to the cerium sub-lattice [14–16]. Thus, upon oxygen vacancy formation in CeO_2, two electrons are left behind, and these localize on the f-level traps of two of the neighbouring Ce atoms, changing their formal valence from Ce(IV) to Ce(III). In Kröger–Vink notation this is

$$O_O^x + 2Ce_{Ce}^x \rightarrow V_O^{\bullet\bullet} + 2Ce_{Ce}' + \tfrac{1}{2}O_2, \qquad (1)$$

where O_O^x is a neutral oxygen on an oxygen lattice site, Ce^x is a neutral cerium in a cerium site, $V_O^{\bullet\bullet}$ is a doubly positively charged vacancy in an oxygen site and Ce_{Ce}' is a singly charged cerium atom in a cerium site. The previously unoccupied 4f state is occupied for the Ce(III) ions, giving the electronic configuration Ce $4f^1$ [17]. UPS and XPS studies have indicated

distinct reduced Ce^{III} states deep in the bandgap of reduced CeO_2 [17].

An explanation for FM behaviour in CeO_2 nanoparticles has been a source of controversy. Oxygen vacancies have been suggested as the relevant defect, and it has been postulated that at the surface, these vacancies induce larger magnetic moments than in the bulk [18]. Conversely, Liu *et al* annealed FM CeO_2 nanostructures in air and under highly reducing conditions, and reported that, regardless of the annealing environment, no ferromagnetic signals were observed. As the authors' photoluminescence (PL) spectra showed characteristic Ce^{III} signals consistent with oxygen vacancy formation, they concluded that oxygen vacancies can not be responsible for FM behaviour in CeO_2 nanoparticles [19]. The authors cite Ce vacancies as a potential FM causing defect [19], although Ce vacancies on the (111) surface have been found to be unfavoured under all conditions relative to oxygen vacancies using first principles methods [20].

A recent LDA + U (U = 7 eV) study of the effect of oxygen vacancy concentration on ferromagnetism in CeO_2 [21] has indicated that as the vacancy concentration increases, the localization behaviour of the excess electrons changes, with significant electron density in the vacancy site. The authors propose that this vacancy site density causes a Ce^{III}–V_O–Ce^{III} superexchange interaction which stabilizes FM ordering [21], causing an increase in ferromagnetism as the vacancy concentration increases. This study, however, also shows some alarming inconsistencies with previous work undertaken on reduced CeO_2. The defect peaks caused by oxygen vacancy formation are split by the Fermi level [21], into occupied and unoccupied states, which is contrary to many previous CeO_2 LDA/GGA + U studies [15, 16, 22]. States in the band gap of reduced ceria are *fully* occupied, and although splitting of defect states may occur, the Fermi level *should* always reside above the defect peaks [22]. Even Ce_2O_3, which can be thought of as CeO_2 with 25% oxygen vacancies is known to be insulating and to slightly prefer *antiferromagnetic* ordering, with no unoccupied defect states between the occupied Ce^{III} states and the unoccupied Ce 4f dominated conduction band [15, 23–25]. The authors also state that vacancy concentrations of 3.13%, 6.25%, 12.5% and 25% were calculated by removing *one* oxygen from a 2 × 2 × 2 (96 atom), 2 × 2 × 1 (48 atom), 2 × 1 × 1 (24 atom) and 1 × 1 × 1 (12 atom) cell respectively [21]. These concentrations would in fact only be true if *Ce vacancies* were being calculated, and so the calculations actually constituted 1.57%, 3.13%, 6.25% and 12.5% oxygen vacancy concentrations.

Here we present a comprehensive DFT analysis of the electronic structure and geometry of oxygen vacancies in 2 × 2 × 2, 2 × 2 × 1, 2 × 1 × 1 and 1 × 1 × 1 cells, together with an examination of spin configurations on the (111), (110) and (100) low index surfaces. We report (i) the complete localization of the excess electrons left behind upon vacancy formation on Ce sites neighbouring the vacancy, with the absence of any significant density in the vacancy site and (ii) the absence of any increased stabilization of FM ordering over antiferromagnetic (AFM) ordering as the concentration of oxygen vacancies is increased and (iii) the difference in energy between FM and AFM behaviour on the low index surfaces is too small to conclude any surface dependence or indeed any definite FM behaviour. Our results clearly show that a mechanism of superexchange mediated by density in the vacancy position can be ruled out, and that oxygen vacancies are not directly involved in any FM behaviour in undoped CeO_2 samples, if such FM behaviour even exists.

2. Methods

All calculations were performed using the projector augmented wave (PAW) implementation within the VASP code [26], and the GGA-PBE [27] exchange–correlation functional. The calculations were performed at a planewave cut off of 500 eV and Monkhorst–Pack [28] k-point meshes of 4 × 4 × 4, 4 × 4 × 2, 4 × 2 × 2 and 2 × 2 × 2 were used for the 1 × 1 × 1, 1 × 1 × 2, 1 × 2 × 2 and 2 × 2 × 2 sized supercells respectively. Due to the well known problems that standard LDA/GGA DFT functionals have in dealing with systems with localized electrons/holes [29–31], we use the GGA +U method [32] to give an improved description of the reduced ceria systems. DFT (LDA/GGA) + U has previously been used to describe oxygen deficient bulk and surfaces of ceria [15, 16, 33] and further to give results in excellent agreement with hybrid DFT [23] and MP2 [34] methods. Two independent studies [35, 25] have attempted to find the optimum U value to use for describing reduced ceria for both LDA + U and GGA + U, and in all cases the optimum U value chosen for LDA + U is 6 eV, with the optimum U value for GGA indicated to be ∼5 eV. This indicates that the U value (U = 7 eV) utilized in the study of Han *et al* [21] *could* have been too large, as U values of greater than 6 eV have been shown to return to a delocalized solution, similar to smaller values of U [35]. This could explain the appearance of density in the vacancy position [21]. The value of U chosen for this GGA study is 5 eV, as this has been shown to give a satisfactory description of reduced CeO_2 [16, 33, 36, 22]. Calculations were deemed converged when the forces on each atom were less than 0.005 eV $Å^{-1}$. The GGA + U calculated lattice constant is 5.48 Å, which is within 1.3% of the experimental lattice constant of 5.41 Å.

3. Localization of the excess electrons in oxygen deficient CeO_2

Analysis of the calculated total and partial (ion decomposed) electronic densities of states (EDOS/PEDOS) for the stoichiometric bulk CeO_2 and for ferromagnetically ordered *single* vacancies in each of the four simulation cells of CeO_2 is shown in figures 1(a)–(e). The defect states in the band gap of all of the reduced cells are *fully* occupied Ce^{III} states, which is at variance with the previous work [21], but consistent with previous theoretical studies [16, 33, 36, 22]. Similarly the antiferromagnetically ordered PEDOS (not shown here) at all concentrations investigated show only fully occupied gap states.

The partial charge density of the defect states for FM and AFM configurations in the 1 × 1 × 1 cell and the 2 × 2 × 2 cell

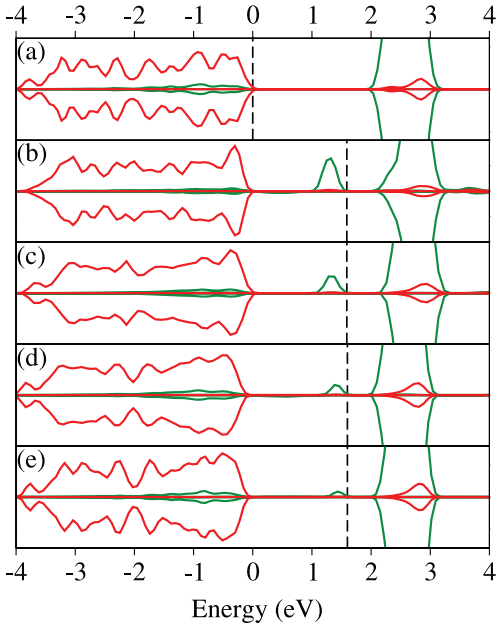

Figure 1. The GGA + U ($U = 5$ eV) calculated PEDOS for (a) stoichiometric bulk, (b) 12.5%, (c) 6.25%, (d) 3.13% and (e) 1.57% FM oxygen deficient bulk CeO_2. (Green indicates Ce 4f states and red O 2p states, colour online only.) The dashed line indicates the highest occupied states. The zero of energy is the valence band maximum in each case.

are shown in figures 2(a)–(d). The excess electrons left behind upon vacancy formation are *clearly* localized on the Ce ions neighbouring the vacancy, formally reducing the Ce^{IV} ions to Ce^{III}. While there is some polarization of the localized Ce^{III} states towards the vacancy, this is similar at both concentration extremes and for both AFM and FM configurations. There is *no* density in the vacancy position, contrary to the results of Han *et al* [21], who reported a density of ∼0.2 e $Å^{-3}$ in the vacancy position for the 1 × 1 × 1 cell. Our charge density analysis, with a maximum of 0.2 e $Å^{-3}$, clearly shows no density in the vacancy position for the same cell for either FM or AFM configurations, figures 2(a) and (b), or in the largest cell, figures 2(c) and (d), with 1 × 2 × 2 and 1 × 1 × 2 showing similar results.

The energy differences between FM and AFM behaviour in the 1.57%, 3.13%, 6.25% and 12.5% oxygen deficient cells are shown in table 1. It is clear from the results, that the energy differences between FM and AFM ordering are *negligible*, with the greatest difference being 1 meV, which indicates no strong preference for either spin configuration. The increased stability of FM versus AFM behaviour (57 meV) as reported by Han *et al* [21] is not seen, with the FM versus AFM differences not changing with increased oxygen vacancy concentration.

4. Ferromagnetism versus antiferromagnetism on the low index surfaces

Many of the reported studies of FM behaviour in CeO_2 have involved nanoscale systems [19, 18]. Size dependent ferromagnetism has been proposed, with nanopowders of under 20 nm showing FM behaviour, and nanopowders above 20 nm not displaying any ferromagnetism [19]. Ceria nanorods have been reported to expose (110) and (100) faces [37], nanoparticles and polycrystalline samples are reported to preferentially expose (111) with a small minority of (100) faces [38], and nanocubes are thought to expose (100) faces [39]. Previous theoretical studies [16, 40] have shown that the ease of oxygen formation energy on the low index surfaces proceeds according to: (110) > (100) > (111). It is therefore of interest to investigate the spin configurations on the low index surfaces to examine if there is any surface sensitivity of FM behaviour. We have therefore computed the formation of oxygen vacancies on the (111), (110) and (100) surfaces of ceria and the resulting spin configurations of the Ce^{III} to clarify if FM behaviour in CeO_2 shows any surface dependence, and to investigate if any density localizes in the surface vacancy positions.

Table 1. Oxygen vacancy formation energies and energy differences between FM and AFM configurations in bulk CeO_2 supercells and low index surfaces. All energies are measured in eV.

CeO_2 bulk cell size	$\Delta E V_O^{\bullet\bullet}$	$E^{FM} - E^{AFM}$
1 × 1 × 1	3.51	−0.001
1 × 1 × 2	2.99	−0.001
1 × 2 × 2	2.65	−0.001
2 × 2 × 2	2.11	−0.001
CeO_2 surfaces	$\Delta E V_O^{\bullet\bullet}$	$E^{FM} - E^{AFM}$
(111)	2.57	0.001
(110) 'simple'	1.93	0.005
(110) 'split'	1.61	0.032
(100)	2.17	−0.001

The (111), (110) and (100) surfaces were cleaved from bulk CeO_2 configurations using the METADISE [41] code, as detailed in earlier CeO_2 surface studies [16, 42], with surface expansions of p(2 × 2) utilized for all surfaces. On the (111) surface it was found that the difference between FM and AFM configurations is negligible, which is consistent with a previous GGA + U study [22]. Two recent studies on the localization of vacancies on the (111) surface of ceria using Hybrid functionals [43] and GGA + U [44] have reported that the excess electrons *do not* wish to localize on the Ce atoms neighbouring the vacancy, but rather on the next nearest neighbour cerium ions, for both surface and subsurface vacancies. We have not calculated the many differing vacancy localization configurations on the (111) surface, as it is unlikely that there will be any FM ordering between more distant atoms, if there is no ordering between the adjacent Ce atoms. Therefore we have investigated *only* the localization of the excess electrons neighbouring the vacancy on the (111) surface. On the (110) we have considered two vacancy configurations, with both configurations having localization on nearest-neighbour Ce ions: (i) the 'simple' vacancy, in which an oxygen is removed and the excess electrons localize on the two cerium ions in the surface layer neighbouring the vacancy, and (ii) the 'split' vacancy, which forms when the oxygen in an adjacent surface row, which is also coordinated to the two surface ceria neighbouring

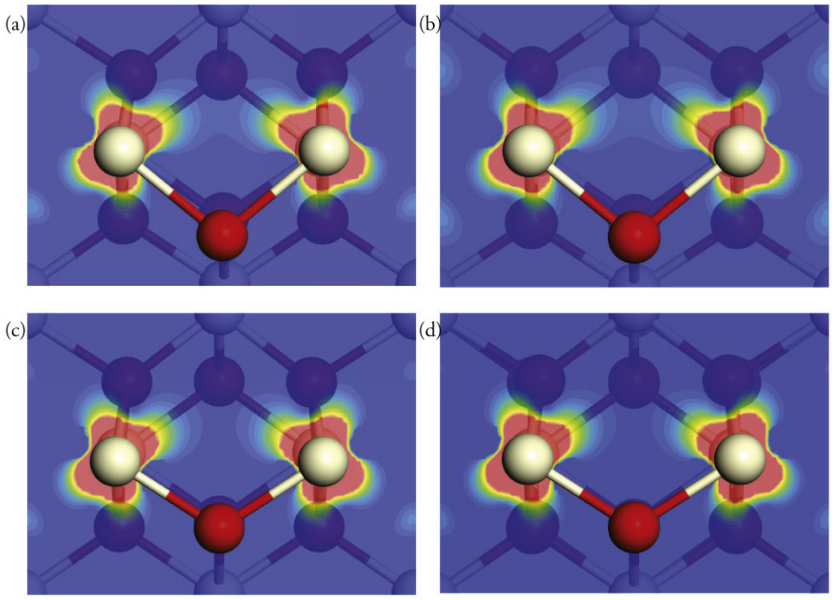

Figure 2. The GGA + U ($U = 5$ eV) partial charge densities for the defect peaks in (a) 12.5% FM, (b) 12.5% AFM, (c) 1.57% FM and (d) 1.57% AFM oxygen deficient bulk CeO_2. Red spheres are oxygen, white spheres are cerium. The contour plots are shown through a plane containing the two reduced Ce^{III} and the vacancy and are plotted from 0 (blue) to 0.2 (red) e $Å^{-3}$.

the vacancy, moves out of the surface to a position almost equidistant between the vacancy site and its original lattice site, figure 3(b). One of the excess electrons then localizes on a surface Ce with the other electron localizing on the subsurface Ce, figure 3(b). This 'split' vacancy configuration has recently been shown to be substantially more stable than the 'simple' vacancy configuration on the (110) surface [45]. In both cases AFM behaviour is *slightly* favoured, with the 'split' vacancy favouring AFM behaviour (by 32 meV) more than the 'simple' vacancy (5 meV). On the (100) surface the energy differences are seen to be negligible, table 1. In all cases, there is no density in the vacancy positions, as indicated in figure 3, which shows the spin density of the two vacancy configurations on the (110) surface.

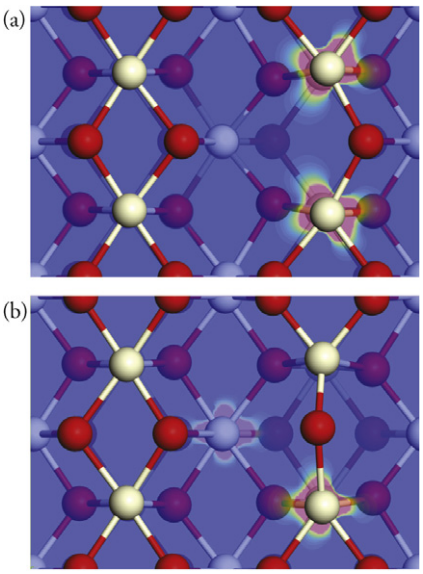

Figure 3. The GGA + U ($U = 5$ eV) calculated spin density for (a) (110) 'simple' and (b) (110) 'split' vacancies. Red spheres are oxygen, white spheres are cerium. The contour plots are shown through a plane parallel to the surface, through the vacancy position, and plotted from 0 (blue) to 0.2 (red) e $Å^{-3}$.

5. Conclusions

Our calculations show that an increase in the oxygen vacancy concentration in bulk Ceria *does not* cause a stabilization of FM versus AFM behaviour. Furthermore our results categorically rule out the appearance of *any* density in the vacancy position as the concentration of vacancies increases. The absence of density in the vacancy position is not a surprise, as ceria is known to *not* behave like a strongly ionic oxide where an F centre can form upon vacancy formation (e.g. MgO) [46]. Instead, the localization of the excess electrons on neighbouring Ce sites is well characterized [46]. Despite this, F centre coupling mechanisms due to oxygen vacancy formation are *still* being proposed as the reason for reported enhanced FM behaviour in CeO_2 samples [11, 47–49]. In fact one study which uses the LDA+U method to investigate oxygen vacancies in CeO_2, reports an F centre mediated mechanism, even though their calculations do not show any density in the vacancy position [47].

Analysis of the surface dependence of vacancy formation and magnetic ordering of the low index surfaces reveals that while vacancies are more favoured on the (100) and (110), the energy differences between FM and AFM are *too small* to indicate FM behaviour on *any* of the surfaces. These results are consistent with the experimental work of Liu *et al*, in which

the authors *reduced* an annealed sample of FM CeO_2 and found that the samples did not exhibit ferromagnetism [19]. In conclusion, our results indicate that oxygen vacancies, in the bulk or on the low index surfaces, do not cause FM behaviour in undoped CeO_2 samples.

Acknowledgments

This work was supported by Science Foundation Ireland through the research frontiers programme (grant numbers 08/RFP/MTR1044 and 09/RFP/MTR2274). Calculations were performed on the IITAC supercomputer as maintained by TCHPC, and the Stokes supercomputer as maintained by ICHEC.

References

[1] Coey J M D and Chambers S A 2008 Oxide dilute magnetic semiconductors—fact or fiction? *MRS Bull.* **33** 1053–8
[2] Dietl T, Ohno H, Matsukura F, Cibert J and Ferrand D 2000 Zener model description of ferromagnetism in zinc-blende magnetic semiconductors *Science* **287** 1019–22
[3] Walsh A, Da Silva J L F and Wei S H 2008 Theoretical description of carrier mediated magnetism in cobalt doped ZnO *Phys. Rev. Lett.* **100** 256401
[4] Sanvito S and Das Pemmaraju C 2009 Comment on 'theoretical description of carrier mediated magnetism in cobalt doped ZnO' *Phys. Rev. Lett.* **102** 159701
[5] Walsh A, Da Silva J L F and Wei S H 2009 Reply to comment on 'theoretical description of carrier mediated magnetism in cobalt doped ZnO' *Phys. Rev. Lett.* **102** 159702
[6] Venkatesan M, Fitzgerald C B and Coey J M D 2004 Unexpected magnetism in a dielectric oxide *Nature* **430** 630
[7] Das Pemmaraju C and Sanvito S 2005 Ferromagnetism driven by intrinsic point defects in HfO_2 *Phys. Rev. Lett.* **94** 217205
[8] Abraham D W, Frank M M and Guha S 2005 Absence of magnetism in hafnium oxide films *Appl. Phys. Lett.* **87** 252502
[9] Coey J M D, Venkatesan M, Stamenov P, Fitzgerald C B and Dorneles L S 2005 Magnetism in hafnium dioxide *Phys. Rev.* B **72** 024450
[10] Hong N H, Sakai J, Poirot N and Brize V 2006 *Phys. Rev.* B **73** 132404
[11] Sundaresan A, Bhargavi R, Rangarajan N, Siddesh U and Rao C N R 2006 Ferromagnetism as a universal feature of nanoparticles of the otherwise nonmagnetic oxides *Phys. Rev.* B **74** 161306
[12] Goodenough J B 2003 Oxide-ion electrolytes *Annu. Rev. Mater. Res.* **33** 91–128
[13] Trovarelli A 2002 *Catalysis by Ceria and Related Materials* (London: Imperial College Press)
[14] Skorodumova N V, Simak S I, Lundqvist B I, Abrikosov I A and Johansson B 2002 Quantum origin of the oxygen storage capability of ceria *Phys. Rev. Lett.* **89** 166601
[15] Fabris S, de Gironcoli S, Baroni S, Vicario G and Gabriele B 2005 Taming multiple valency with density functionals: a case study of defective ceria *Phys. Rev.* B **71** 041102(R)
[16] Nolan M, Grigoleit S, Sayle D C, Parker S C and Watson G W 2005 Density functional theory studies of the structure and electronic structure of pure and defective low index surfaces of ceria *Surf. Sci.* **576** 217–29
[17] Henderson M A, Perkins C L, Engelhard M H, Thevuthasan S and Peden C H F 2003 Redox properties of water on the oxidized and reduced surface of CeO_2(111) *Surf. Sci.* **526** 1–18
[18] Ge M Y, Wang H, Liu E Z, Liu J F, Jiang J Z, Li Y K, Xu Z A and Li H Y 2008 On the origin of ferromagnetism in CeO_2 nanocubes *Appl. Phys. Lett.* **93** 062505
[19] Liu Y, Lockman Z, Aziz A and MacManus-Driscoll J 2008 Size dependent ferromagnetism in cerium oxide (CeO_2) nanostructures independent of oxygen vacancies *J. Phys.: Condens. Matter* **20** 165201
[20] Zhang C, Michaelides A, King D A and Jenkins S J 2008 Structure of gold atoms on stoichiometric and defective ceria surfaces *J. Chem. Phys.* **129** 194708
[21] Han X, Lee J and Yoo H I 2009 Oxygen-vacancy-induced ferromagnetism in CeO_2 from first principles *Phys. Rev.* B **79** 100403(R)
[22] Zhang C, Michaelides A, King D A and Jenkins S J 2009 Oxygen vacancy clusters on ceria: decisive role of cerium f electrons *Phys. Rev.* B **79** 075433
[23] Da Silva J L F, Ganduglia-Pirovano M V, Sauer J, Bayer V and Kresse G 2007 Hybrid functionals applied to rare earth oxides: the example of ceria *Phys. Rev.* B **75** 045121
[24] Skorodumova N V, Ahuja R, Simak S I, Abrikosov I A, Johansson B and Lundqvist B I 2001 Electronic, bonding and optical properties of CeO_2 and Ce_2O_3 from first principles *Phys. Rev.* B **64** 115108
[25] Andersson D A, Simak S I, Johansson B, Abrikosov I A and Skorodumova N V 2007 Modeling of CeO_2, Ce_2O_3, and CeO_{2-x} in the LDA + U formalism *Phys. Rev.* B **75** 035109
[26] Kresse G and Hafner J 1994 *Ab initio* molecular-dynamics simulation of the liquid-metal–amorphous-semiconductor transition in germanium *Phys. Rev.* B **49** 14251–71
[27] Perdew J P, Burke K and Ernzerhof M 1996 Generalized gradient approximation made simple *Phys. Rev. Lett.* **77** 3865
[28] Monkhorst H J and Pack J D 1976 Special points for brillouin-zone integration *Phys. Rev.* B **13** 5188–92
[29] Scanlon D O, Walsh A, Morgan B J and Watson G W 2008 An *ab initio* study of reduction of V_2O_5 through the formation of oxygen vacancies and Li intercalation *J. Phys. Chem.* C **112** 9903–11
[30] Scanlon D O, Walsh A, Morgan B J, Nolan M, Fearon J and Watson G W 2007 Surface sensitivity in lithium-doping of MgO: a density functional theory study with correction for on-site Coulomb interactions *J. Phys. Chem.* C **111** 7971–9
[31] Morgan B J, Scanlon D O and Watson G W 2009 Small polarons in Nb- and Ta-doped rutile and anatase TiO_2 *J. Mater. Chem.* **19** 5175–8
[32] Dudarev S L, Botton G A, Savrasov S Y, Humphreys C J and Sutton A P 1998 Electron-energy-loss spectra and the structural stability of nickel oxide: a LSDA + U study *Phys. Rev.* B **57** 1505
[33] Nolan M, Parker S C and Watson G W 2005 The electronic structure of oxygen vacancy defects at the low index surfaces of ceria *Surf. Sci.* **595** 223–32
[34] Herschend B, Baudin M and Hermansson K 2006 CO adsorption on CeO_2 (110) using hybrid-DFT embedded-cluster calculations *Chem. Phys.* **328** 345–53
[35] Castleton C W M, Kullgren J and Hermansson K 2007 Tuning LDA + U for electron localization and structure at oxygen vacancies in ceria *J. Chem. Phys.* **127** 244704
[36] Galea N M, Scanlon D O, Morgan B J and Watson G W 2009 A GGA + U study of the reduction of ceria surfaces and their partial reoxidation through NO_2 adsorption *Mol. Simul.* **35** 577–83
[37] Zhou K, Wang X, Sun X, Peng Q and Li P 2005 Enhanced catalytic activity of ceria nanorods form well defined reactive crystal planes *J. Catal.* **229** 206–12
[38] Aneggi E, Llorca J, Boaro M and Trovarelli A 2005 Surface-structure sensitivity of CO oxidation over polycrystalline ceria powders *J. Catal.* **234** 88–95

[39] Si R and Flytzani-Stephanopoulos M 2008 Shape and crystal-plane effects of nanoscale ceria on the activity of Au–CeO_2 catalysts for the water–gas shift reaction *Angew. Chem. Int. Edn* **47** 2884–7

[40] Nolan M, Parker S C and Watson G W 2006 CeO_2 catalysed conversion of CO, NO_2 and NO from first principles energetics *Phys. Chem. Chem. Phys.* **8** 216

[41] Watson G W, Kelsey E T, de Leeuw N H, Harris D J and Parker S C 1996 Atomistic simulation of disclocations, surfaces and interfaces in MgO *J. Chem. Soc.: Faraday Trans.* **92** 433–8

[42] Nolan M, Parker S C and Watson G W 2006 Reduction of NO_2 on ceria surfaces *J. Phys. Chem.* B **110** 2256

[43] Ganduglia-Piravano M V, Da Silva J L F and Sauer J 2009 Density-functional calculations of the structure of near-surface oxygen vacacnies and electron localization on CeO_2 *Phys. Rev. Lett.* **102** 026101

[44] Li H Y, Wang H F, Gong Z Q, Guo Y L, Giuo Y, Lu G and Hu P 2009 Multiple configurations of the two excess 4f electrons on defective CeO_2(111): origin and implications *Phys. Rev.* B **79** 193401

[45] Scanlon D O, Galea N M, Morgan B J and Watson G W 2009 The reactivity on the (110) surface of ceria: a GGA + U study of surface reduction and the adsorption of Co and NO_2 *J. Phys. Chem.* C **113** 11095–103

[46] Ganduglia-Pirovano M V, Hofmann A and Sauer J 2007 Oxygen vacancies in transition metal and rare earth oxides: current state of understanding and remaining challenges *Surf. Sci. Rep.* **62** 219–70

[47] Song Y Q, Zhang H W, Wen Q Y, Peng L and Xiao J Q 2008 Direct evidence of oxygen vacancy mediated ferromagnetism of Co doped CeO_2 thin films on Al_2O_3(0001) substrates *J. Phys.: Condens. Matter* **20** 255210

[48] Song Y Q, Zhang H W, Yang Q H, Liu Y L, Li Y X, Shah L R, Zhu H and Xiao J Q 2009 Electronic structure and magnetic properties of Co-doped CeO_2: based on first principle calculation *J. Phys.: Condens. Matter* **21** 125504

[49] Wen Q W, Zhang H W, Song Y W, Yang Q H, Zhu H and Xiao J Q 2007 Room-temperature ferromagnetism in pure and Co doped CeO_2 powders *J. Phys.: Condens. Matter* **19** 246205